

High Resolution X-ray Spectroscopy and the Nature of Warm Absorbers in AGN

Julian H. Krolik

Department of Physics and Astronomy, Johns Hopkins University, Baltimore MD 21218 USA

Abstract. Although soft X-ray absorption features in AGN were discovered almost ten years ago, the nature and location of the gas creating them has remained controversial. However, by making use of the newly-available high-resolution spectra provided by *XMM-Newton* and *Chandra*, we should be able to make substantial advances. The first such spectra indicate that multiple ionization states coexist in the absorber; this is a natural consequence of photoionization physics. Photoionized evaporation in the presence of a copious mass source locks the ratio of ionizing intensity to pressure to a critical value. A broad range of temperatures can all coexist in equilibrium for this value of the ratio of ionizing intensity to pressure. Consequently, the flow is expected to be strongly inhomogeneous in temperature. The inferred distance of this material from the source of ionizing radiation depends on how much matter exists at the highest-obtainable temperature. This distance can be measured by monitoring how ionic column densities respond to changes in the ionizing continuum on timescales of days to years.

In ROSAT-data, the spectral resolution and signal/noise were so poor that the only feature strong enough to be seen was the O K-edge, and the ionization state of O could be determined only roughly. Labelling ionization level by the ionization parameter $\xi \equiv L_{ion}/nr^2$ (where L_{ion} is conventionally defined as the luminosity between 1 and 1000 Ryd, n is the H-nucleus density, and r is the distance to the source of radiation), this sort of data was capable only of identifying the presence of matter with $\xi \lesssim 30$, and perhaps distinguishing ionization parameters at the highest end of this range from those an order of magnitude or more smaller.

Unfortunately, ROSAT was totally incapable of detecting any matter more strongly ionized because higher ionization destroys OVIII. Other elements' K-edges could not be seen in ROSAT data either because their energy was outside its limited range (e.g., Fe) or because their abundance was too small to permit detection with such crude data. To put this (semi)-quantitatively, in gas with solar abundances most of whose O has not been stripped, O K-edges were detectable by ROSAT when the column density $N \gtrsim 10^{21} \text{ cm}^{-2}$. Even if the ROSAT energy range extended to the K-edge of ionized Fe at 7–9 keV, a column density almost three orders of magnitude larger would have been necessary in order for a significant edge to have been formed. In this sense, ROSAT-level data was roughly 1000 times less sensitive to highly-ionized than to weakly-ionized gas.

Data of the sort produced by ASCA was better, but not greatly. Although its resolution and signal/noise were good enough to permit estimates of the depths of the OVII and OVIII edges separately (e.g., Reynolds et al. 1995), it could see no other edge features reliably. The next-deepest K-edges (Si, S, Ar, etc.) are so much smaller in opacity that they would be detectable in ASCA data only for much greater absorbing columns. In principle, ASCA's nominal energy range included the Fe K-edge, but the effective area there was so small as to make searching for this edge impractical. Thus, like ROSAT, ASCA could detect matter with $\xi \lesssim 30$, but could improve upon ROSAT by permitting $\xi \simeq 30$ to be distinguished from, say, $\xi = 3$. Again like

1. The Unanswered Questions about Warm Absorbers: How *Chandra* and *XMM* Can Help

Although absorption features due to highly-ionized species were first clearly seen in AGN spectra taken with ROSAT almost ten years ago (Turner et al. 1993), most of the fundamental facts about them remain obscure today. This is true at even the most basic, empirical level.

1.1. The ionization distribution

For example, we do not even know which ionization states are present in the absorbing gas. Because increasing levels of ionization tend to move atomic features higher in energy and then remove them altogether, the character of ionization states possible to see in X-ray spectra is strongly influenced by the specifics of instrumentation. Consequently, our efforts to determine how much matter there is in which ionization state suffer from extremely strong instrumental selection effects.

ROSAT, it was effectively blind to more highly-ionized matter.

The advent of the grating spectrometers on *Chandra* and *XMM* has already dramatically changed this frustrating situation, and will undoubtedly improve matters further in the near future. Their tremendously finer spectral resolution permits study of line transitions, not just edges, while their much greater signal/noise allows one to search for much weaker features. With data of this quality, it is possible to search for species expected to be common up to $\xi \sim 1000$ even when the column density of that gas is as small as $\lesssim 10^{21} \text{ cm}^{-2}$ —and we are starting to find them. Several different recent warm absorber studies employing grating data report that more than one ionization component is detected, with ξ ranging anywhere from a few tens to ~ 1000 (Kaastra et al. 2000, Collinge et al. 2001, Kaspi et al. 2001).

Thus, in the next few years we may reasonably hope to make much progress on the most basic empirical question of warm absorber studies: measuring the distribution $dN/d\xi$.

1.2. Location and origin

After identifying the absorber’s ionization state, the next obvious question is where to place it in the AGN system. Proposed distances have ranged all the way from inside or near the broad-line region at 0.01 – 0.1 pc from the nucleus (Reynolds et al. 1995, George et al. 1998, Netzer et al. 2001) to many tens of pc away in the narrow-line region (Bottorff et al. 2000). Some have argued that there is absorbing material across this entire range of radii (Otani et al. 1996, Morales et al. 2000). Others (e.g., Krolik & Kriss 1995) have argued that the absorbing gas should be identified with the scattering region posited by Seyfert galaxy unification schemes, perhaps ~ 1 pc from the nucleus when $L_{\text{ion}} \sim 10^{44} \text{ erg s}^{-1}$.

The state of affairs regarding the absorbing matter’s origin is even worse. A few of the diverse suggestions that have been floated include: evaporation off “bloated stars” in the broad-line region (Netzer 1996); gas evaporated off the torus obscuring the nucleus (Krolik & Kriss 1995); and a wind driven off the accretion disk (Elvis 2000; Bottorff et al. 2000). The absorbing gas’s ultimate fate has been left wholly unconsidered.

This, too, is a topic on which we may hope for enlightenment from new spectroscopy data. As has been remarked in numerous papers (Reynolds et al. 1995, Krolik & Kriss 2001, Netzer et al. 2001), variability in absorption features can strongly constrain the location of the gas responsible. The virtue of the new data sets is that, by making so many features observable, our odds of seeing variability in one or more of them are greatly improved. Moreover, because the new data are less subject to ionization selection effects (as discussed in the previous sub-

section), the location bounds placed by variability can be applied more generally.

1.3. Kinematics

Independent of where the absorbing gas is located, we’d also like to know which way it’s moving. For this issue, high-resolution spectroscopy is essential. If the absorbing gas possesses ions with ionization potentials ~ 1 keV (as is necessary to have numerous soft X-ray features), its temperature cannot be much greater than $\sim 10^7$ K. Transonic motions at this temperature would then be $\sim 300 \text{ km s}^{-1}$ or slower. It immediately follows that spectral resolution $\Delta E/E \gtrsim 1000$ is a prerequisite for beginning to detect motions at this speed.

Because resolution of this caliber is exactly what *Chandra* and *XMM* have now delivered, we are beginning to learn about this question. Kaspi et al. (2001), for example, have shown that the absorber in NGC 3783 is moving toward us (relative to the nucleus) at $\simeq 500 \text{ km s}^{-1}$.

1.4. Geometry

Although the depth of an edge may tell us the total column density of ions along the line of sight, it does not tell us whether they are all clumped together, or spread out smoothly, or clustered at a variety of locations. And, of course, absorption tells us nothing about the existence of matter along other directions.

Other constraints are necessary to make progress answering questions of this sort. For example, resonance line emission components offset toward the red from absorption components are the classic signature of outflows. The relative equivalent width of the emission and absorption components reveals the ratio between the mean optical depth on lines of sight other than ours to the ratio on the line toward us. Similarly, the relative velocity widths further constrain the gas’s geometric disposition. Making use of the emission/absorption equivalent width indicator, Kaspi et al. (2001) have already suggested that the absorbing gas in NGC 3783, while occupying a large part of solid angle around the nucleus, does not completely cover it.

Clumpiness in the gas can be analyzed in any of several ways, given quality spectroscopy: Emission lines that are either collisionally-excited or created by recombination yield measurements of the gas’s emission measure; combined with independent density estimates, one can then infer the total emitting volume and compare it to the available volume in the region. Alternatively, spectroscopic data that requires gas at several different ionization levels co-existing in more or less the same location would strongly suggest a clumpy, inhomogeneous environment.

1.5. Dynamics

Given our ignorance about the warm absorber’s kinematics, location, and origin, it should come as no surprise that almost nothing is known with confidence about its dynamics. We have as yet advanced hardly at all past listing the “usual suspects”: gravity, thermal pressure gradients (Balsara & Krolik 1993), radiation pressure (Chelouche & Netzer 2001, Morales & Fabian 2002), and magnetic fields (Bottorff et al. 2000).

2. Warm Photoionized Equilibria

To make further progress, it is helpful to consider a few constraints imposed by the basic facts of photoionization physics. We begin with the most elementary of these, a relationship that links the ionization parameter, the distance, the gas column density, and its volume filling factor. From the definition of ξ and the fact that the column density $N = n\Delta r$, where Δr is the total distance along the line of sight occupied by the absorbing gas, we immediately see (as shown by Turner et al. 1993) that

$$r = \frac{L_{ion}}{N\xi} \frac{\Delta r}{r}. \quad (1)$$

Because $\Delta r/r$ cannot possibly be greater than unity, the inferred ionization parameter and column density of an absorber, when combined with the luminosity of the ionizing source, place an upper bound on its distance from that source:

$$r \leq r_{max} \equiv \frac{L_{ion}}{N\xi}. \quad (2)$$

For typical numbers, $r_{max} \sim 30L_{ion,44}N_{22}^{-1}(\xi/100)^{-1}$ pc. Here we have scaled the ionizing luminosity to 10^{44} erg s $^{-1}$ and the column density to 10^{22} cm $^{-2}$. For fixed r_{max} , the more highly clumped the gas is, the smaller the radius at which it might be found.

A second constraint is provided by the nature of photoionization equilibrium. If the gas’s cooling time is shorter than the time required for it flow through the absorbing region, we can expect that it is in energy balance with the radiation. If that is the case, its temperature is a unique function of its ionization parameter ξ .

If we wish to link photoionization physics with fluid dynamics, it is more convenient to write the ionization parameter in a related, but significantly different form: $\Xi \equiv \xi/(4\pi ckT)$. The factor of $4\pi ck$ makes Ξ dimensionless; more significantly, by dividing by the temperature, a given Ξ at any particular radius corresponds to a certain pressure. Viewed from the opposite perspective, if the boundary condition is a fixed pressure and the gas is in energy balance, Ξ is determined, but T is uniquely determined only when $T(\Xi)$ is single-valued. Although $T(\xi)$ is, in general, unique, when the ionizing continuum has a form typical of AGN, $T(\Xi)$, in general, is *multi-valued*

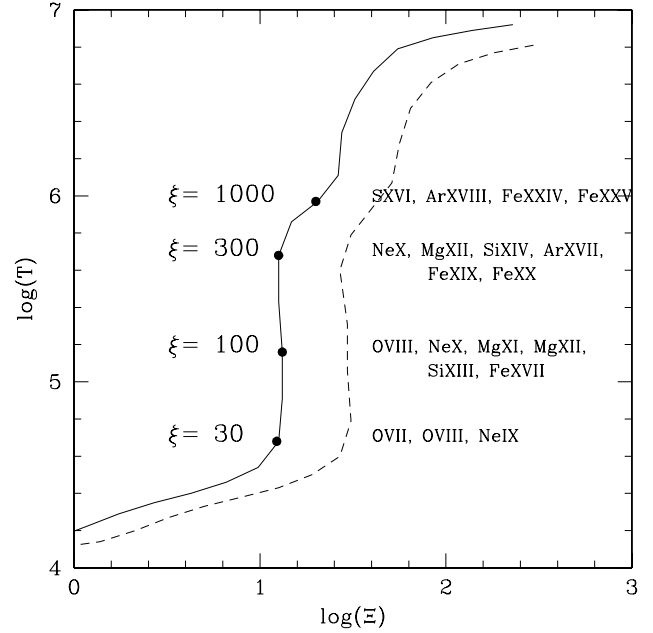


Fig. 1. The temperature equilibrium curve for two guesses (Krolik & Kriss 2001—solid curve, Kaspi et al. 2001—dashed curve) about the unknown shape of the EUV spectrum in Seyfert galaxies. Although the value of Ξ at which the nearly vertical rise between 5×10^4 K and 1×10^6 K takes place depends on the shape of the spectrum, the character of the rise is a persistent feature of all reasonable AGN spectra. The location of several values of ξ is shown, as are a few of the dominant ionization stages associated with each of the marked values.

in the range of temperatures between $\simeq 5 \times 10^4$ K and $\gtrsim 10^6$ K (Krolik, McKee & Tarter 1981; fig. 1). As a result, the boundary conditions may not suffice to determine the temperature; its history (and possibly the influence of thermal instabilities) is instead the final deciding factor. The fact that the thermal balance may be multi-valued is central to the study of warm absorbers because the multiple-valued solutions occur in exactly the range of conditions capable of making soft X-ray features.

When a detailed calculation is made of the thermal equilibrium curve, it is necessary to make several guesses about matters that we don’t truly know and yet have noticeable effect on the result. The distribution of elemental abundances is the first of these. Generally-speaking, solar abundances are assumed; other choices can alter the detailed shape of the curve, but within quite wide bounds have at most modest effect on the shape of $T(\Xi)$. More important to the thermal balance curve is the shape of the ionizing continuum. In low-redshift objects, we can observe the continuum at energies just below 1 Rydberg and again above $\simeq 500$ eV, but the most important segment of the ionizing continuum is precisely in the band from 13 eV to $\simeq 500$ eV that we can never directly see.

The best we can do is smoothly interpolate from either side. Fortunately, as shown in Figure 1, different plausible guesses do not result in qualitatively different results. Both equilibrium calculations shown in the figure were based on continuum shapes meant to apply to the Seyfert galaxy NGC 3783 (one in Kaspi et al. 2001, the other in Krolik & Kriss 2001). Although rather different, both predict the same general sort of behavior—a nearly vertical rise in temperature from $\simeq 5 \times 10^4$ K to almost 10^6 K. The value of Ξ where this takes place is called Ξ_c .

In fact, it is worthwhile to focus greater attention on the “vertical branch” of the photoionized thermal equilibrium curve because it is significant for several reasons. The first, as just mentioned, is that the range of ξ inferred from the ionization stages seen in warm absorber spectra is $\sim 10 - 1000$; this is almost exactly the range traversed on the vertical branch. In other words, if warm absorbers are in a state of photoionization equilibrium and thermal balance, they “live” on the vertical branch.

Second, the vertical branch has a rather special thermodynamic property: it is marginally stable to isobaric thermal perturbations. Were $dT/d\Xi > 0$, constant pressure perturbations would be stable because increasing the temperature from an initial point on the equilibrium curve must result in net cooling; conversely, were $dT/d\Xi < 0$, the same sort of perturbation grows exponentially because the excursion causes net heating. However, on the vertical branch $d\Xi/dT = 0$: in this case, if the temperature is perturbed while the pressure is fixed, the gas remains in a state of zero net radiative energy gain or loss. Consequently, there is no temperature “feedback”, either positive or negative. Perturbations are neither strongly damped nor strongly amplified—they simply do whatever the outside agency creating them demands. Although it is true that the curve of thermal balance can never be precisely vertical, to the extent that it is nearly so, the net cooling or heating that is engendered by the perturbations is small, and the magnitude of growth permitted in a region of weak instability is capped at a low level as a new segment of the equilibrium curve is quickly reached.

Third, far from being a special case, the value of Ξ at which the vertical branch occurs is actually a preferred value of the pressure-based ionization parameter. Whenever large amounts of cool material are exposed to a strong ionizing flux (as might readably be imagined near an AGN), the low-density portion of this cool matter finds itself rapidly ionized and heated. If the heating time is short compared to the flow time, the ambient pressure rises equally rapidly. At fixed distance from the source of ionizing radiation, this means the value of Ξ surrounding the cool matter rapidly falls. Nothing stops this fall in Ξ until it reaches Ξ_c , where the net energy exchange via radiation switches from heating to cooling. Similarly, if the pressure overshoots to the net-cooling side of the vertical branch, matter cools rapidly, losing pressure, until balance is achieved—at exactly Ξ_c .

This portion of the argument may be summed up very simply: Given that, by definition, warm absorbers are exposed to AGN fluxes, it makes sense to suppose that they are photoionized. Let us suppose for the moment that the gas is in photoionization equilibrium and radiative balance. Then the particular ions observed (OVII,VIII; NeX; MgXII; SiXIV; etc.) indicate that the gas lies on the vertical branch of the $T(\Xi)$ curve. Because that branch allows a wide range of temperatures to coexist at a single pressure, it follows that the material is likely to contain multiple sub-regions whose temperature could be anywhere within the range found on the vertical branch of the equilibrium curve. Moreover, pressure balance tends to force photoionized gases in the presence of a copious mass source toward Ξ_c . That is, it is a natural consequence of photoionization physics that we should see gas with $\Xi = \Xi_c$ and that it should be inhomogeneous in temperature.

3. Global Picture

These special thermodynamic properties of the vertical branch find a natural application in the context of AGN warm absorbers. These are frequently seen in type 1 Seyfert galaxies, a variety of AGN in which we have excellent reason to believe that extremely optically thick obscuring matter wraps around the nucleus with roughly toroidal geometry (Antonucci 1993, Krolik 1999). Where the ionizing radiation of the nucleus strikes the inner edge of the obscuring stuff, exactly the process described in the previous paragraph can be expected to take place: copious amounts of matter should be ionized and heated, maintaining $\Xi \simeq \Xi_c$. Until the temperature rises quite high, the heating time is far shorter than the flow time: as shown in detail in Krolik & Kriss (2001), if the flow speed is of the magnitude observed ($\simeq 500 \text{ km s}^{-1}$), this criterion is met for $T < 4 \times 10^6 r_{pc}^{-1/2}$ K, for r_{pc} the distance from the central source in parsecs.

As the newly-liberated material is heated, it will expand in order to maintain pressure balance. One might then ask, “Will the expanding parcels eventually be confined? Or will they spread out and fill the entire volume of the region?” Suppose that the matter we see by its “warm absorber” features is clumpy. If the volume outside the clumps has lower pressure, the clumps will expand at roughly their internal sound speeds. The ratio in column density between the low-pressure background and the high-pressure absorbing lumps may then be estimated as

$$N_{bkgd}/N_{abs} \sim (r/\Delta r_{abs})(c_s/v_{flow}), \quad (3)$$

where the absorber has radial thickness Δr_{abs} and sound speed c_s . Because the sound speed at $\sim 10^5$ K (the typical temperature inferred for warm absorber regions) is $\sim 50 \text{ km s}^{-1}$, it is clear that the column density of the background is *automatically* close to the column density of the absorber if there is strong clumping. That is, one

must expect the background to be a significant part of the absorbing structure. Put yet another way, it is probably best to consider the entire system as volume-filling, albeit one that is likely to be strongly inhomogeneous.

Although the ionization parameter Ξ is tightly constrained by photoionized thermodynamics, the temperature, at least within the range permitted at $\Xi \simeq \Xi_c$, is hardly constrained at all. We should expect, then, that the evaporating matter in this region might exist anywhere in the temperature range $5 \times 10^4 - \sim 10^6$ K, i.e., $30 \lesssim \xi \lesssim 1000$. The issue is not “What is the favored value of T or ξ ?”, but “What is the distribution of T and ξ within this broad range?” Small accidents having to do with irregularities in the source of matter (the obscuring torus?) or “bumps” in the outflow of heated gas could affect this distribution, so different objects could easily differ in detail.

At fixed pressure, the hottest regions have the least density and so, per unit mass, occupy the largest volume. For this reason, one might expect most of the volume to be occupied by relatively hot gas, but it is likely studied by smaller regions of higher density and lower temperature. Each of these sub-regions can easily change its temperature over time.

4. Implications

This conceptual picture has numerous implications for the character of warm absorbers. The most basic, of course, is that the features we see should originate in ions found in photoionized equilibrium over a span of a factor of 20 or so in temperature. There are also other, more quantitative implications.

4.1. Location

Returning to equations 1 and 2, we can rewrite them as

$$r \simeq r_{max}(\xi_{max}) = \frac{L_{ion}}{\xi_{max} N(\xi_{max})}, \quad (4)$$

where ξ_{max} is the highest ξ (corresponding to the highest T) attainable in a flow time. Because the gas at ξ_{max} is the hottest that we can expect to find in the absorber region, it should occupy the largest part of the volume. That is, for the hottest gas $\Delta r/r \simeq 1$, while cooler gas is strongly clumped. Scaled in terms of typical numbers, the predicted distance

$$r \simeq 3 \frac{L_{ion,44}}{N_{22}} \text{ pc}, \quad (5)$$

where ξ_{max} has been set at 1000.

A few parsecs is, of course, the scale of the inner torus (as seen, for example, in near-infrared imaging—Thatte et al. 1997, Marco & Alloin 2000—or H₂O maser spots—Greenhill et al. 1996). It is likewise the expected scale of the polarizing reflection region that permits us to see type 1 Seyfert nuclei in type 2 Seyfert galaxies.

4.2. Dynamics

With an estimate of the distance to the nucleus, the strength of gravity may be more quantitatively estimated. Making use of equation 5, we find that the free-fall speed in the absorber region is $\simeq 30(L/L_E)^{-1/2} N_{22}^{1/2}$ km s⁻¹. Here L_E is the Eddington luminosity and we have supposed that most of the bolometric luminosity is in the ionizing band. Because the sound speed in the hottest phase of the absorber is ~ 100 km s⁻¹, we can expect that thermal pressures alone may be able to drive an outflow unless $L/L_E \ll 1$. Whether radiation or magnetic forces supplement the thermal pressure gradient remains an open question, but the fact that we see blue-shifted absorption lines indicating an outflow should now be no surprise.

4.3. Geometry

If the warm absorber is formed by this sort of photoionized evaporation off the inner edge of the obscuring torus, the torus itself blocks the warm gas from expanding to the side. A biconical expansion and outflow results. For this reason, we might expect the warm absorber to occupy fully only a part of solid angle around the nucleus. Moreover, depending on our viewing angle, parts of the obscuring matter might block our view of selected portions of the far side of the outflow. Thus, emission line equivalent widths should indicate substantial, but incomplete, solid angle coverage—as is tentatively seen in NGC 3783 (Kaspi et al. 2001).

4.4. Variability and location

This picture also makes specific predictions about variability in absorption features. The column densities we see are, of course, controlled by ionization balance in the line-of-sight gas. The governing equation can be written (in abridged form) as

$$\frac{d \ln n_i}{dt} = \frac{n_{i-1}}{n_i} F'_x \sigma'_{ion} + n_e \alpha''_{rec} \frac{n_{i+1}}{n_i} + \dots \quad (6)$$

$$- F_x \sigma_{ion} - n_e \alpha_{rec} - \dots \quad (7)$$

where the density of ionization stage i is n_i , $i \pm 1$ correspond to the stages once more or less ionized, F_x is the photon flux at the relevant ionization edge, σ_{ion} is the appropriately averaged ionization cross section, and the primes and double primes denote the quantities relevant to the $i + 1$ and $i - 1$ ionization stages. When $n_{i+1} \gg n_i$ (as is often true for the particular ionization stages seen), two terms dominate the rest, so that

$$\frac{d \ln n_i}{dt} \simeq n_e \alpha''_{rec} n_{i+1}/n_i - F_x \sigma_{ion}. \quad (8)$$

The characteristic time for effecting changes in the absorbing column is then

$$t_{ion} \sim 10^{6 \pm 1} \frac{r_{pc}^2}{L_{ion,44}} \text{ s}. \quad (9)$$

Different species have varying ionization timescales, depending on the details of their atomic structures. For example, if one examines the more abundant species in the relevant ionization conditions, SiXIV, FeXXV, and FeXXVI tend to have longer ionization times, while OVI and the ions around FeXX tend to have somewhat shorter timescales. The range is not terribly large, however: the ± 1 in the exponent in equation 9 more or less comprises the range for the species of greatest interest (Krolik & Kriss 2001).

Timescales of days to years are, of course, very convenient timescales for human observations. Because we know which species should vary on which timescales (parameterized by the ionizing flux in the absorbing region), monitoring spectroscopy should be a very powerful tool for constraining the location and conditions of the absorbing gas.

4.5. How would the warm absorber look when seen from the side?

Finally, it is striking how much the warm absorber region resembles the reflection region that allows us to see the nuclei of type 2 Seyfert galaxies. Both regions appear to lie at distances \sim pc; both are highly-ionized; both are flowing outward at speeds of several hundred km s^{-1} ; the total column densities in both are $\sim 10^{22} - 10^{23} \text{ cm}^{-2}$. It would appear to make a great deal of sense to suppose that they are the same structure, simply viewed at different angles.

References

- Antonucci, R.R.J. 1993, *Ann. Revs. Astron. Astrop.* 31, 473
 Balsara, D. & Krolik, J.H. 1993, *Ap.J.* 402, 109
 Bottorff, M., Korista, K. & Shlosman, I. 2000, *Ap.J.* 537, 134
 Chelouche, D. & Netzer, H. 2001, *M.N.R.A.S.* 326, 916
 Collinge, M. et al. 2001, *Ap.J.* 557, 2
 Elvis M., *Ap.J.* 545, 63
 George, I. M., Turner, T. J., Netzer, H., Nandra, K., Mushotzky, R. F., & Yaqoob, T. 1998, *ApJS*, 114, 73
 Greenhill, L.J., Gwinn, C.R., Antonucci, R. & Barvainis, R. 1996, *Ap.J. Letts.* 472, L21
 Kaastra, J. S., Mewe, R., Liedahl, D. A., Komossa, S., Brinkmann, A. C. 2000, *Astron. Astrop.*, 354, L83
 Kaspri, S., Brandt, W. N., Netzer, H., George, I., Chartas, G., Behar, E., Sambruna, R., Garmire, G. P. & Nousek, J. A. 2001, *Ap.J.* 554, 216
 Krolik, J.H. 1993, *Active Galactic Nuclei: From the Central Black Hole to the Galactic Environment* (Princeton: Princeton University Press)
 Krolik, J. H., & Kriss, G. A. 1995, *ApJ*, 447, 512
 Krolik, J. H., & Kriss, G. A. 2001, *ApJ* 561, 684
 Krolik, J.H., McKee, C.F. & Tarter, C.B. 1981, *Ap.J.* 249, 422
 Marco, O. & Alloin, D. 2000, *Astron. Astrop.* 353, 465
 Morales, R.F., Fabian, A.C., & Reynolds, C.S. 2000, *M.N.R.A.S.* 315, 149
 Morales, R.F. & Fabian, A.C. 2002, *M.N.R.A.S.* 329, 209

Netzer, H. 1996, *Ap.J.* 473, 781

Netzer, H. et al., *astro-ph/0112027*

Otani, C., et al. 1996, *P.A.S.J.* 48, 211

Reynolds, C.S., Fabian, A.C., Nandra, K., Inoue, H., Kunieda, H., Iwasawa, K. 1995, *M.N.R.A.S.* 277, 901

Thatte, N., Quirrenbach, A., Genzel, R., Maiolino, R. & Tecza, M. 1997, *Ap.J.* 490, 238

Turner, T.J., Nandra, K., George, I.M., Fabian, A.C. & Pounds, K. 1993, *Ap.J.* 419, 127